Supporting information

Facile one-pot synthesis of defect-engineered step-scheme WO$_3$/g-C$_3$N$_4$ heterojunctions for efficient photocatalytic hydrogen production

Xiya Du[#, a], Song Song[#, a], Yating Wang[*, c], Wenfeng Jin[a], Tong Ding[a], Ye Tian[a] and Xingang Li[*, a, b]

[a] *Collaborative Innovation Center of Chemical Science and Engineering (Tianjin), State Key Laboratory of Chemical Engineering, Tianjin Key Laboratory of Applied Catalysis Science and Engineering, School of Chemical Engineering and Technology, Tianjin University, Tianjin 300072, P. R. China.*

[b] *School of Chemical and Biological Engineering, Lanzhou Jiaotong University, Lanzhou, 730070, P. R. China.*

[c] *Tianjin Key Laboratory of Brine Chemical Engineering and Resource Eco-utilization, School of Chemical Engineering and Material Science, Tianjin University of Science & Technology, Tianjin 300457, P. R. China.*

[*]Corresponding author
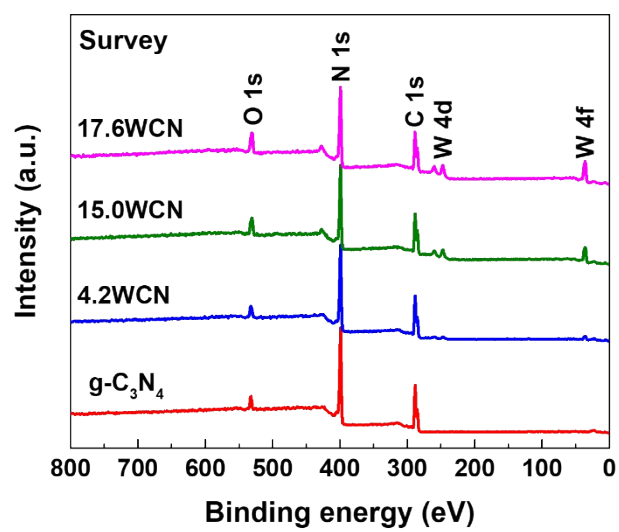
Email: xingang_li@tju.edu.cn
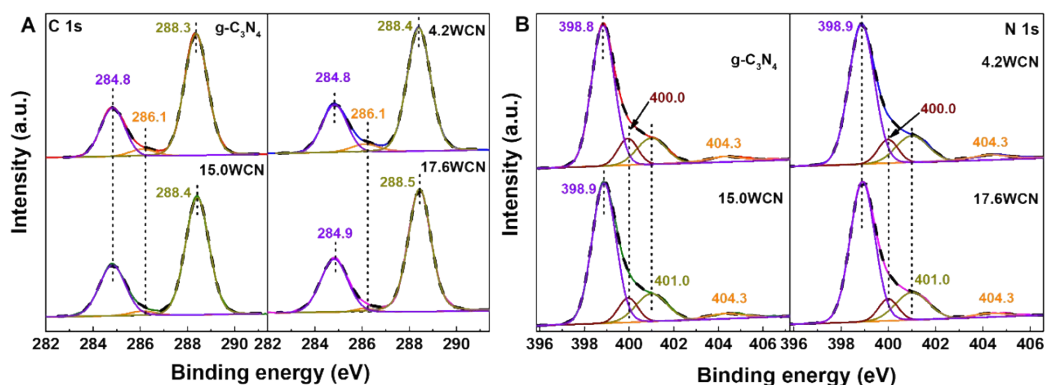
Fig. S1. XPS survey spectra of g-C$_3$N$_4$ and nWCN.

Fig. S2. XPS spectra of (A) C 1s and (B) N 1s.

The C 1s XPS spectra of g-C_3N_4 in Fig. S2A could be divided into three peaks at 284.8 eV, 286.1 eV and 288.3eV, ascribing to the carbon impurities species (C-C), the C-N and sp^2-hybridized carbon bonded to the neighboring three nitrogen atoms (N−C=N) in g-C_3N_4 lattice, respectively.[1] Compared with g-C_3N_4, the peaks locating at about 284.8 eV and 288.3eV in the *n*WCN samples have a certain shift toward high binding energy. Fig. S2B displays the N 1s spectra of g-C_3N_4 and *n*WCN. It can be segregated into four peaks at 398.8 eV, 400.0 eV, 401.0 eV and 404.3 eV, corresponding to sp^2-hybridized N species (C=N−C), sp^3-hybridized tertiary N−(C)$_3$ groups, amino functional groups (C−N−H) and the π-excitation of C-N heterocycles, respectively.[2, 3] The peak at 398.8 eV of *n*WCN has a slight positive shift compared with pure g-C_3N_4. Combined with the C 1s XPS spectra, the shift to high binding energy indicates the existence of charge transfer between g-C_3N_4 and WO_3.[4]
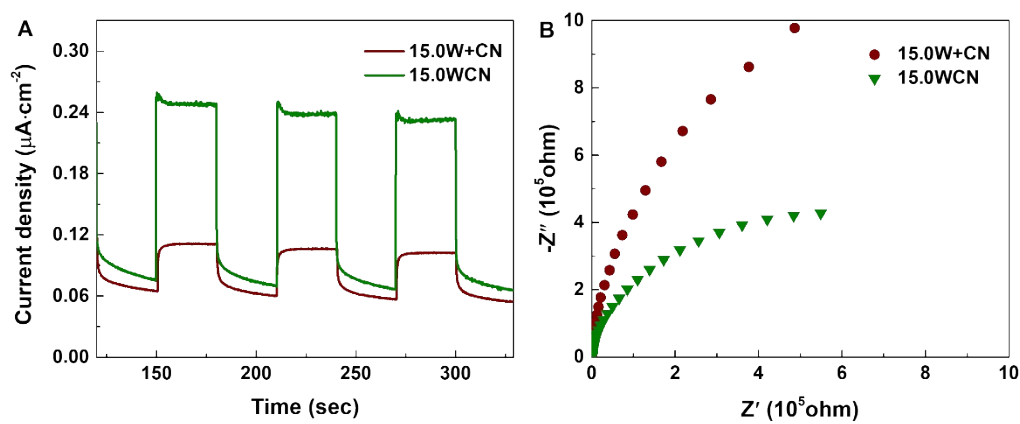
Fig. S3. (A) Transient photocurrent responses and (B) EIS Nyquist plots of

15.0W+CN and 15.0WCN.

4
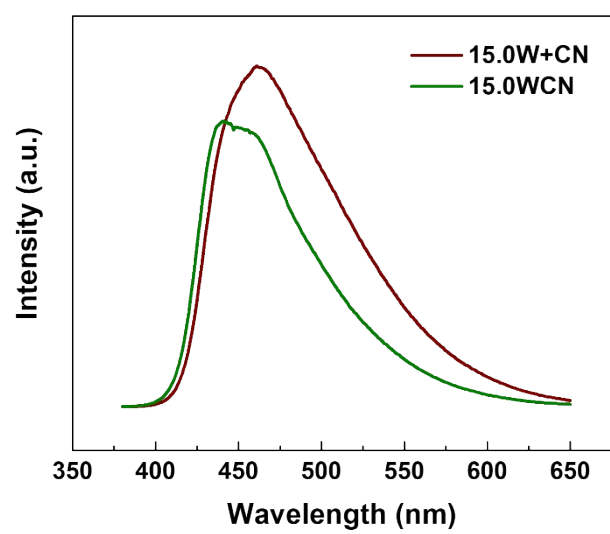
Fig. S4. Photoluminescence emission spectra of 15.0W+CN and 15.0WCN.

Table S1. The BET surface area and pore structure of the samples.

Samples	S_{BET} (m^2 g^{-1})	Pore volume (cm^3 g^{-1})	Pore diameter (nm)
WO$_3$	4.2	0.01	2.1
g-C$_3$N$_4$	14.8	0.03	4.8
4.2WCN	16.7	0.04	4.7
15.0WCN	18.8	0.03	4.7
17.6WCN	19.1	0.04	4.7

Table S2. The H_2 production rates and apparent quantum efficiencies of the samples.

Samples	H_2 production rate (μmol h^{-1})	AQE (%)
g-C$_3$N$_4$	5.8	1.7%
4.2WCN	11.2	3.3%
15.0WCN	24.5	7.4%
17.6WCN	12.4	3.7%

Table S3. Binding energy, peak area and relative percentage of different W species in W 4f spectra.

samples	Binding energy of W (eV)				peak area (Counts)		Percentage (%)	
	W^{6+}		W^{5+}		W^{6+}	W^{5+}	W^{6+}	W^{5+}
	$4f_{5/2}$	$4f_{7/2}$	$4f_{5/2}$	$4f_{7/2}$				
WO_3	38.0	35.9	-	-	112734.6	-	100	0
4.2WCN	37.3	35.2	36.3	34.2	3135.0	153.6	95.3	4.7
15.0WCN	37.4	35.3	36.3	34.3	13635.3	781.8	94.6	5.4
17.6WCN	37.4	35.3	36.4	34.3	18890.6	819.4	95.8	4.2

Table S4. Binding energy, peak area and relative percentage of different O species in O 1s spectra.

samples	Binding energy of O 1s (eV)			peak area (Counts)			Percentage (%)		
	O_L	O_{OH}	O_{C-O}	O_L	O_{OH}	O_{C-O}	O_L	O_{OH}	O_{C-O}
WO_3	530.7	531.8	-	61148.0	14720.9	-	80.6	19.4	-
4.2WCN	529.9	531.8	532.5	2263.7	4432.4	7381.9	16.1	31.5	52.4
15.0WCN	529.9	531.8	532.5	8087.6	6732.2	3749.4	43.5	36.3	20.2
17.6WCN	530.0	531.8	532.5	11673.1	6000.6	3506.7	55.1	28.3	16.6

Equation S1: $\alpha h\nu = A(h\nu - E_g)^{\frac{2}{n}}$

where α, hν, A and E_g are the optical absorption coefficient, the photon energy, the absorption constant and the band gap energy, respectively. The value of n is determined by the transition properties of semiconductor. The n equals to 1for the direct transition, while the n equals to 4 for the indirect transition.[5] Hence, the values of n are 1 and 4 for WO_3 and $g\text{-}C_3N_4$, respectively.

Equation S2: $I_t = A\exp\left(\frac{-t}{\tau}\right) + y_0$

Equation S3: $I_t = A_1\exp\left(\frac{-t}{\tau_1}\right) + A_2\exp\left(\frac{-t}{\tau_2}\right)$

Where the A_1 and A_2 are constants representing the weight factor. The τ_1 and τ_2 are fast decay time and slow decay time, which stem from the nonradiative recombination of photo-generated electrons at CB into the trap sites of defects and radiative recombination of the photogenerated electrons with the holes at VB, respectively.[6] The PL lifetime of WO_3 was obtained using single exponential fitting equation (Equation S2), while the PL lifetimes of $g\text{-}C_3N_4$ and nWCN were calculated using double exponential fitting equation (Equation S3). We also calculated the average fluorescence lifetime τ using the Equation S4.

Equation S4: $\tau = A_1\tau_1^2 + A_2\tau_2^2/A_1\tau_1 + A_2\tau_2$

References

[1] C. Liu, H. Huang, W. Cui, F. Dong and Y. Zhang, *Appl. Catal. B: Environ.*, 2018, **230**, 115-124.

[2] L. Shi, L. Liang, F. Wang, M. Liu, K. Chen, K. Sun, N. Zhang and J. Sun, *ACS Sustain. Chem. Eng.*, 2015, **3**, 3412-3419.

[3] J. Fu, C. Bie, B. Cheng, C. Jiang and J. Yu, *ACS Sustain. Chem. Eng.*, 2018, **6**, 2767-2779.

[4] J. Fu, Q. Xu, J. Low, C. Jiang and J. Yu, *Appl. Catal. B: Environ.*, 2019, **243**, 556-565.

[5] T. Xiao, Z. Tang, Y. Yang, L. Tang, Y. Zhou and Z. Zou, *Appl. Catal. B: Environ.*, 2018, **220**, 417-428.

[6] M. Wu, T. Ding, J. Cai, Y. Wang, H. Xiang, H. Zhang, Y. Tian, T. Zhang and X. Li, *ACS Sustain. Chem. Eng.*, 2018, **6**, 8167-8177.